550.385.4

ANALYTICAL MODEL TO STUDY THE BEHAVIOUR OF AURORAL PARTICLES IN A LOCAL REGION OF THE MAGNETOTAIL AT THE ONSET OF A MAGNETOSPHERIC SUBSTORM

by

R.J. PELLINEN
Division of Geomagnetism, Finnish Meteorological Institute, Helsinki, Finland

Abstract

Basing on observations that a substorm often begins in a small local time sector, a model is assumed in which the neutral sheet current is diverted around a small disturbed region. A simple assumption is that the current varies linearly with distance from the centre of the disturbance in the x direction in a solar-magnetospheric (SM) coordinate system, and that the diverted current is channeled within narrow paths δ_y wide on the dawn and dusk sides of the disturbed area. The vector potential integrals of the assumed current pattern and the corresponding electric and magnetic field components are evaluated analytically. The introduction of the disturbance current loop into the magnetotail results in a magnetic field structure in which new neutral lines of the X and O types can be observed; these are connected to each other in a continuous neutral ring on the xy equatorial plane. The magnetic and electric field components around the neutral regions are given. It is demonstrated that this type of field structure is capable of accelerating particles to high energies owing to linear and betatron mechanisms. The model formulation reveals electric field components along the magnetic field lines. Field-aligned acceleration in a typical substorms situation is demonstrated with an example of electron energization from 1 keV to 21 keV in 1.1 seconds. The model is further tested by taking typical values of the defined parameters based on observations within the magnetotail. The induced electric field is found to be comparable to the average cross-tail electrostatic field, and it may well be orders of magnitude greater. The model agrees with present observations on the onset phenomena.

1. *Introduction*

In a series of publications (HEIKKILA and PELLINEN [10], PELLINEN and HEIKKILA [16], PELLINEN [15]) we have developed a theoretical model to describe phenomena during the onset of magnetospheric substorms. This paper gives technical details on the calculations involved in developing the model.

The construction of the model is based on the following empirical data:

a) The onset of the expansion phase of a magnetospheric substorm is characterized by sudden localized changes in a small region of the magnetotail (ROSTOKER and CAMIDGE [17]).
b) Most observations made with magnetometers carried on spacecraft show magnetic fluctuations in the magnetotail.
c) Bursts of particles, electrons and protons with energies up to one MeV or more have been reported, generally in association with magnetispheric substorm activity (HONES *et al.* [11], SARRIS *et al.* [18], [19], TERASAWA and NISHIDA [20], KIRSCH *et al.* [13], BAKER and STONE [3]).
d) Field-aligned currents have been observed at the onset of a substorm. These are associated with the precipitation regions of auroral particles (ARNOLDY [2]), which have been extensively studied optically (*e.g.* FUKUNISHI [9]).
e) Large-scale convective plasma flows, both earthward and tailward, have been observed during magnetospheric substorms. Their velocities seldom exceed 1000 km/s (HONES *et al.* [12], FRANK *et al.* [7]).

Present knowledge on auroral phenomena has been taken into account in addition to the above observations (*e.g.* the similarity of simultaneous auroral forms over both hemispheres).

The following results of theoretical works have also been used:

a) Self-consistent calculations show that the neutral-sheet current is carried by plasma sheet particles on closed field lines, due mainly to curvature drift and partly to gradient drift (BIRD and BEARD [5]).
b) The cross-tail current is diverted along the magnetic field lines as a Birkeland current down to the ionosphere, where it is carried along by a westward electrojet (BOSTRÖM [6]).

Basing on the results summarized above, onset phenomena can be discussed qualitatively and significant conclusions can be reached, but no mathematical model can be derived. However, a mathematical model for current perturbation (HEIKKILA and PELLINEN [10]) is needed for detailed calculations, and we have chosen a very simple one in which the cross-tail current in a local region of the neutral sheet grows linearly from the centre of the disturbance, and the current lines are closed by narrow sheet currents in the x direction at the border of the disturbance (Fig-

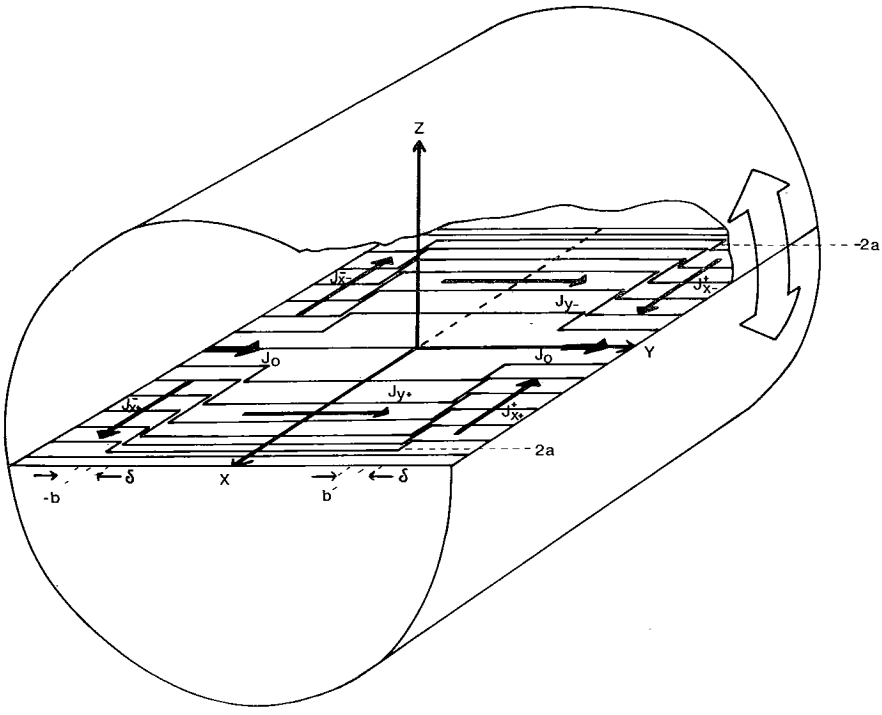

Figure 1. Geometry of the magnetotail current, with a time-dependent diversion of the neutral sheet current around a localized bubble.

ures 1 and 2). This model is based on three main assumptions (PELLINEN [15]).

1) The displacement current is disregarded because it is several orders of magnitude smaller than the particle current (HEIKKILA and PELLINEN [16]).
2) the perturbation is restricted to the plane of the neutral sheet, *i.e.* $\delta J_z = 0$, $\delta J_x = -\delta J_y$
3) there are no disturbances in the currents outside the rectangular disturbed area in Figure 1.

The disturbance is limited to the area $-a \leqslant x \leqslant +a$ and $-b \leqslant y \leqslant +b$, and grows with the velocities $\pm v_x$ along the x axis and $\pm v_y$ along the y axis. In our coordinate system the x axis points towards the earth, y axis towards dusk, and z axis northwards. The origin is located at the centre of the disturbance. We define the current densities in a local region of the neutral sheet as follows

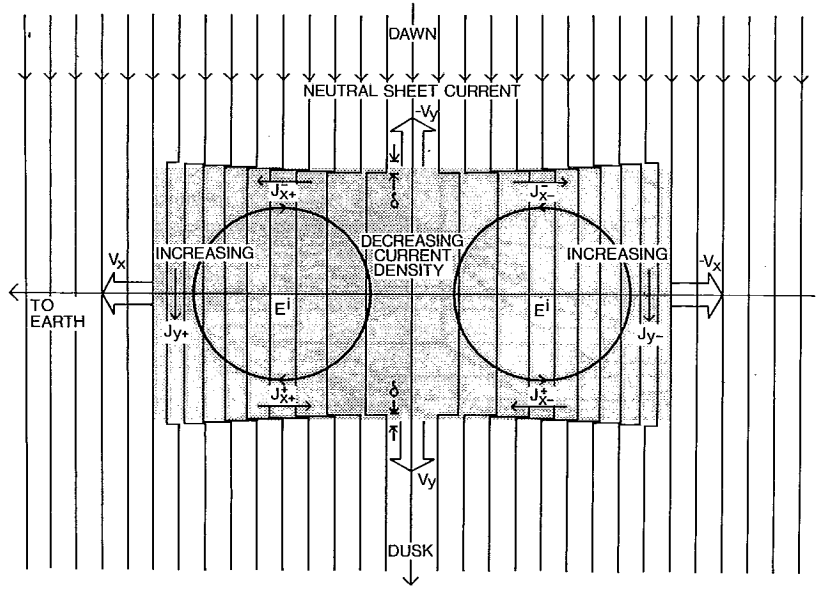

Figure 2. In our mathematical ad-hoc model, the disturbance is assumed to be rectangular in shape, with linearly increasing amplitude and size.

$$J_{y+} = J_o + \frac{jx}{a} - j\,, \qquad 0 \leqslant x \leqslant 2a;\ |y| \leqslant b$$

$$J_{y-} = J_o - \frac{jx}{a} - j\,, \qquad -2a \leqslant x \leqslant 0;\ |y| \leqslant b \tag{1.1}$$

$$J_y = J_o\,, \qquad |x| > 2a \quad \text{or} \quad |y| > b$$

where J_o is the cross-tail current density and j the current disturbance.

We assume that the accompanying x-directed currents are limited to narrow regions of width δ where $y = \pm b$. The current density is assumed to be constant over δ. Basing on the continuity equation for the currents we can write

$$J_{x+}^{\pm} = \mp \frac{jx}{\delta}\left(1 - \frac{x}{2a}\right)\,, \qquad 0 \leqslant x \leqslant 2a$$

$$J_{x-}^{\pm} = \mp \frac{jx}{\delta}\left(1 + \frac{x}{2a}\right)\,, \qquad -2a \leqslant x \leqslant 0 \tag{1.2}$$

The parameters a, b, and j defining the geometry of the current density distribution are dependent on time.

The current perturbation, (1.1) and (1.2), has a vector potential $\bar{A}(\bar{r},t)$, which can be used to estimate the disturbed magnetic field from $\nabla \times \bar{A}(\bar{r},t)$. To study the tail phenomena, this magnetic field must be added vectorially to an appropriate tail field that closely corresponding to the situation at breakup, with a thin plasma sheet and stretched tail-like structure. BIRD and BEARD [5] have derived a suitable field model with a thin neutral sheet current that varies slowly in strength with distance down the tail. This field model and the disturbed field are described and matched in section 2.

According to our assumption, the disturbance grows continuously during the onset. This leads to a temporal development of the vector potential, and hence to and induced electric field that can be calculated from the equation $\bar{E}^i = -\partial\bar{A}(\bar{r},t)/\partial t$. The regions in which the magnetic field drops to zero are of interest when considering the energization of charged particles (TERASAWA and NISHIDA [20]). We will discuss these regions in section 3 and the energization in section 4.

The forms of $\bar{E}^i$ and disturbed $\bar{B}$ are rather complicated. Numerical treatment is easiest with a computer. The treatment and representation of the parameters may create some problems. This is discussed in section 5.

Our model will be discussed in section 6.

2. *Disturbed magnetic field in the magnetotail*

The vector potential of the current perturbation is

$$\bar{A}(\bar{r},t) = \frac{\mu_0}{4\pi} \int_{\tau'} \frac{\bar{J}(\bar{r}',t)}{|\bar{r} - \bar{r}'|} \, d\tau' \tag{2.1}$$

The total vector potential for the tail current system can be written as:

$$\bar{A} = \bar{A}_r + (A_o + A_{y+} + A_{y-})\hat{y} + (A^+_{x+} + A^-_{x+} + A^+_{x-} + A^-_{x-})\hat{x} \, . \tag{2.2}$$

$\bar{A}_r + A_o\hat{y}$ is the unperturbed part, where $\bar{A}_r$ is due to the rest of the circuit; and must be evaluated before the total magnetic field can be specified.

The integrals in the proposed current system of equation (2.1) can be evaluated analytically, as stated by MURPHY *et al.* [14]. After inserting equations (1.1) and (1.2) in (2.1), we get

$$A^{\pm}_{x+} = \mp \frac{\mu_0}{16\pi}\frac{j}{a}\Big\{C^{\mp}(4a - \xi - 3x) - [2x^2 - (y \mp b)^2 - z^2 - 4ax]$$
$$\ln(2C^{\mp} + 2\xi - 2x)\Big\}^{\xi_1 = 2a}_{\xi_2 = 0}$$

$$A^{\pm}_{x-} = \mp \frac{\mu_0}{16\pi}\frac{j}{a}\Big\{C^{\mp}(4a + \xi + 3x) + [2x^2 - (y \mp b)^2 - z^2 - 4ax] \tag{2.3}$$
$$\ln(2C^{\mp} + 2\xi - 2x)\Big\}^{\xi_2 = 0}_{\xi_3 = -2a}$$

and

$$A_{y\pm} = \frac{\mu_0}{4\pi}\frac{j}{a}\Big\{\frac{g}{2}[\ln(Q_1Q_2/g) + 1] - \frac{1}{4}(Q_1^2 + Q_2^2) + f_1Q_1 + f_2Q_2$$
$$+ (x \mp a)[\xi\ln(Q_1Q_2/g) + f_1\ln(\xi + l_1) + f_2\ln(\xi + l_2) \tag{2.4}$$
$$- 2z(\tan^{-1}U_1 + \tan^{-1}U_2 + \tan^{-1}(\xi/z))]\Big\}^{\xi = \pm 2a - x}_{\xi = -x}$$

Some expressions in these formulas are abreviated as follows:

$$C^{\mp} = [(x - \xi)^2 + (y \mp b)^2 + z^2]$$

$$f_1 = b + y, \quad f_2 = b - y, \quad g = \xi^2 + z^2, \quad l_i = (g + f_i^2)^{1/2}$$

$$Q_i = f_i + l_i, \quad U_i = (Q_i - \xi)/z \quad \text{and} \quad i = 1 \text{ or } 2.$$

The next step is to calculate the magnetic field created by the disturbance current j. The equation

$$\bar{B} = \nabla \times \bar{A} \tag{2.5}$$

gives

$$\bar{B} = \Big(-\frac{\partial A_y}{\partial z}\Big)\hat{x} + \frac{\partial A_x}{\partial z}\hat{y} + \Big(\frac{\partial A_y}{\partial x} - \frac{\partial A_x}{\partial y}\Big)\hat{z}$$
$$= B_x\hat{x} + B_y\hat{y} + B_z\hat{z} \tag{2.6}$$

After straightforward but lengthy calculations we get

$$B_x = \frac{\mu_0 j}{4\pi}\frac{1}{a}\Big\{z\ln\Big[\frac{Q_{13}^2Q_{23}^2}{Q_{14}Q_{24}Q_{15}Q_{25}}\frac{g_4g_5}{g_3^2}\Big] + 2x\Big[\tan^{-1}U_{14} + \tan^{-1}U_{15} - 2\tan^{-1}U_{13}$$
$$+ \tan^{-1}U_{24} + \tan^{-1}U_{25} - 2\tan^{-1}U_{23} + \tan^{-1}\Big(\frac{S_4}{z}\Big) + \tan^{-1}\Big(\frac{S_5}{z}\Big)$$
$$- 2\tan^{-1}\Big(\frac{S_3}{z}\Big)\Big] - 2a\Big[\tan^{-1}U_{14} + \tan^{-1}U_{24} + \tan^{-1}\Big(\frac{S_4}{z}\Big) - \tan^{-1}U_{15}$$
$$- \tan^{-1}U_{25} - \tan^{-1}\Big(\frac{S_5}{z}\Big)\Big]\Big\} \tag{2.7}$$

$$B_y = \frac{\mu_0 j}{4\pi}\frac{z}{a}\Big\{\frac{1}{2}\ln\frac{K_{24}K_{25}K_{13}^2}{K_{14}K_{15}K_{23}^2} - \frac{a}{2}[C_{24} - C_{14} - C_{25} + C_{15}]$$
$$+ \frac{3x}{4}[C_{24} - C_{14} + C_{25} - C_{15} - 2C_{23} + 2C_{13}]$$
$$+ ax[C_{14}K_{14} - C_{24}K_{24} - C_{15}K_{15} + C_{25}K_{25}]$$
$$- \frac{R_1}{4}[C_{14}K_{14} + C_{15}K_{15} - 2C_{13}K_{13}]$$
$$+ \frac{R_2}{4}[C_{24}K_{24} + C_{25}K_{25} - 2C_{23}K_{23}]\Big\} \tag{2.8}$$

$$B_z = \frac{\mu_0 j}{4\pi}\cdot\frac{1}{a}\Big\{f_1\ln\frac{K_{13}^2}{K_{14}K_{15}} + f_2\ln\frac{K_{23}^2}{K_{24}K_{25}} - 2z\Big[\tan^{-1}U_{14} + \tan^{-1}U_{15}$$
$$- 2\tan^{-1}U_{13} + \tan^{-1}U_{24} + \tan^{-1}U_{25} - 2\tan^{-1}U_{23} + \tan^{-1}\Big(\frac{S_4}{z}\Big)$$
$$+ \tan^{-1}\Big(\frac{S_5}{z}\Big) - 2\tan^{-1}\Big(\frac{S_3}{z}\Big)\Big] + x\ln\Big[\frac{Q_{13}^2Q_{23}^2}{Q_{14}Q_{15}Q_{24}Q_{25}}\frac{g_4g_5}{g_3^2}\Big]$$
$$+ a\ln\Big[\frac{Q_{14}Q_{24}g_5}{Q_{15}Q_{25}g_4}\Big] + \frac{f_1}{4}\Big[2\ln\frac{K_{14}K_{15}}{K_{13}^2} - 2a(C_{14} - C_{15})$$
$$+ 3x(C_{14} + C_{15} - 2C_{13}) + R_1(C_{14}K_{14} + C_{15}K_{15} - 2C_{13}K_{13})$$
$$- 4ax(C_{14}K_{14} - C_{15}K_{15})\Big] + \frac{f_2}{4}\Big[2\ln\frac{K_{24}K_{25}}{K_{23}^2} - 2a(C_{24} - C_{25})$$
$$+ 3x(C_{24} + C_{25} - 2C_{23}) + R_2(C_{24}K_{24} + C_{25}K_{25} - 2C_{23}K_{23})$$
$$- 4ax(C_{24}K_{24} - C_{25}K_{25})\Big]\Big\} \tag{2.9}$$

where

$$S_3 = -x, \quad S_4 = 2a - x, \quad S_5 = -2a - x, \quad l_{ij} = (g_j + f_i^2)^{1/2}$$
$$g_i = S_i^2 + z^2, \quad R_i = 2x^2 - f_i^2 - z^2, \quad Q_{ij} = f_i + (g_j + f_i^2)^{1/2}$$
$$U_{ij} = \frac{1}{z}[Q_{ij} - S_j], \quad C_{ij} = [S_j^2 + f_i^2 + z^2]^{-1/2}, \quad K_{ij} = [C_{ij}^{-1} + S_j]^{-1}$$

To investigate the effects of introducing such a perturbation to the magnetotail, we have chosen the simple tail model used by BEARD *et al.* [4], with a thin neutral sheet current whose strength decreases slowly with distance down the tail. The tail model modified for our purposes is:

$$B_x = 2\pi J_0 \sqrt{\frac{x_0}{x}}\, \theta(z) \tag{2.10}$$

where

$$\theta(z) = +1, \quad \text{when } z > 0$$
$$\theta(z) = -1, \quad \text{when } z < 0$$
$$\theta(z) = 0, \quad \text{when } z = 0$$

$$B_r = -\frac{wJ_0}{x}\sqrt{\frac{x_0}{x}}\left(\cos\theta - \frac{r}{w}\sin\theta\cos\theta \tanh^{-1}\frac{2rw\sin\theta}{w^2+r^2}\right.$$
$$\left. -\pi\frac{r}{w}\cos^2\theta + \frac{w^2 - r^2 + 2r^2\cos^2\theta}{2rw}\tan^{-1}\frac{2rw\cos\theta}{w^2 - r^2}\right) \tag{2.11}$$

$$B_\theta = -\frac{wJ_0}{x}\sqrt{\frac{x_0}{x}}\left(-\sin\theta - \frac{w^2 - r^2 + 2r^2\cos^2\theta}{2rw}\tanh^{-1}\frac{2rw\sin\theta}{w^2+r^2}\right.$$
$$\left. + \frac{r}{w}\sin\theta\cos\theta\left[\pi - \tan^{-1}\frac{2rw\cos\theta}{w^2 - r^2}\right]\right) \tag{2.12}$$

B_r and B_θ can be transformed to cartesian coordinates B_y and B_z with the following transformation forms.

$$B_y = B_r\sin\theta + B_\theta\cos\theta, \quad \sin\theta = \frac{y}{\sqrt{y^2+z^2}}$$
$$B_z = B_r\cos\theta - B_\theta\sin\theta, \quad \cos\theta = \frac{z}{\sqrt{y^2+z^2}} \tag{2.13}$$

where J_0 is the current in the neutral sheet, on its inner edge x_0.

3. *Induced electric field*

The vector potential (2.1) has three time-dependent parameters a, b and j. Temporal changes in the vector potential result in an induced electric field:

$$\bar{E}_i = -\frac{\partial j}{\partial t}\frac{\partial \bar{A}}{\partial j} - \frac{\partial a}{\partial t}\frac{\partial \bar{A}}{\partial a} - \frac{\partial b}{\partial t}\frac{\partial \bar{A}}{\partial b} \tag{3.1}$$

The first term corresponds to the changes in the current density, the second to the tailward movement of the conducting plasma, and the last to the east-to-west movement of the disturbance. In our current system, $a = a(t)$, $b = b(t)$, so

$$\frac{\partial a}{\partial t} = \frac{da}{dt} = \frac{v_x}{2} \qquad \text{and} \qquad \frac{\partial b}{\partial t} = \frac{db}{dt} = v_y$$

$$E_x = -\frac{\partial j}{\partial t}\frac{\partial A_x}{\partial j} - \frac{v_x}{2}\frac{\partial A_x}{\partial a} - v_y\frac{\partial A_x}{\partial b}$$

$$E_y = -\frac{\partial j}{\partial t}\frac{\partial A_y}{\partial j} - \frac{v_x}{2}\frac{\partial A_y}{\partial a} - v_y\frac{\partial A_y}{\partial b} \tag{3.2}$$

Starting again from equations (2.3) and (2.4), we receive

$$\begin{aligned}
E_x = \frac{\mu_0}{16\pi a}\Bigg\{ & \left(-\frac{\partial j}{\partial t} + \frac{v_{xj}}{2a}\right)\Bigg[3x(2l_{13} - 2l_{23} - l_{14} + l_{24} - l_{15} + l_{25}) \\
& + 2a(l_{14} - l_{24} - l_{15} + l_{25}) - 4ax\ln\frac{K_{14}K_{25}}{K_{24}K_{15}} - R_1\ln\frac{K_{13}^2}{K_{14}K_{15}} \\
& + R_2\ln\frac{K_{23}^2}{K_{24}K_{25}}\Bigg] - \frac{jv_x}{2}\Bigg[2S_4(2x - S_4)(C_{24} - C_{14}) \\
& - 2S_5(2x - S_5)(C_{25} - C_{15}) + 2(l_{14} - l_{24} + l_{25} - l_{15}) \\
& - 4x\ln\frac{K_{14}K_{25}}{K_{15}K_{24}} + 2(2x^2 - z^2 - 4ax)(C_{24} - C_{14}) \\
& - 2(2x^2 - z^2 + 4ax)(C_{25} - C_{15}) - 2f_1^2(C_{15} - C_{14}) + 2f_2^2(C_{25} - C_{24})\Bigg] \\
& - jv_y\Bigg[f_1\Big\{C_{14}(2a - 3x) - C_{15}(2a + 3x) + 6xC_{13} - 2\ln\frac{K_{14}K_{15}}{K_{13}^2} \\
& - R_1(K_{14}C_{14} + K_{15}C_{15} - 2K_{13}C_{13})
\end{aligned}$$

$$+ 4ax\,(K_{14}C_{14} - K_{15}C_{15})\Big\}$$

$$+ f_2\Big\{C_{24}(3x-2a) + C_{25}(3x+2a) - 6xC_{23} + 2\ln\frac{K_{24}K_{25}}{K_{23}^2}$$

$$+ R_2(K_{24}C_{24} + K_{25}C_{25} - 2K_{23}C_{23})$$

$$- 4ax\,(K_{24}C_{24} - K_{25}C_{25})\Big\}\Big]\Big\} \tag{3.3}$$

Similarly E_y can be written as:

$$E_y = \frac{\mu_0}{4\pi a}\Big\{\Big(-\frac{\partial j}{\partial t} + \frac{v_{xj}}{2a}\Big)\Big\{\frac{g_4}{2}\ln(Q_{14}Q_{24}/g_4) + \frac{g_5}{2}\ln(Q_{15}Q_{25}/g_5)$$

$$- g_3\ln(Q_{13}Q_{23}/g_3) + \frac{g_4}{2} + \frac{g_5}{2} - g_3$$

$$+ \frac{1}{4}(2Q_{13}^2 + 2Q_{23}^2 - Q_{14}^2 - Q_{24}^2 - Q_{15}^2 - Q_{25}^2)$$

$$- f_1(2Q_{13} - Q_{14} - Q_{15}) - f_2(2Q_{23} - Q_{24} - Q_{25})$$

$$- x\Big[2S_3\ln(Q_{13}Q_{23}/g_3) - S_4\ln(Q_{14}Q_{24}/g_4) - S_5\ln(Q_{15}Q_{25}/g_5)$$

$$+ f_1\ln\frac{K_{14}K_{15}}{K_{13}^2} + f_2\ln\frac{K_{24}K_{25}}{K_{23}^2}\Big]$$

$$+ 2zx\Big[2\tan^{-1}U_{13} + 2\tan^{-1}U_{23} + 2\tan^{-1}\Big(\frac{S_3}{z}\Big)$$

$$- \tan^{-1}U_{14} - \tan^{-1}U_{24} - \tan^{-1}\Big(\frac{S_4}{z}\Big)$$

$$- \tan^{-1}U_{15} - \tan^{-1}U_{25} - \tan^{-1}\Big(\frac{S_5}{z}\Big)\Big]$$

$$- a\Big[S_4\ln(Q_{14}Q_{24}/g_4) - S_5\ln(Q_{15}Q_{25}/g_5)$$

$$+ f_1\ln\frac{K_{15}}{K_{14}} + f_2\ln\frac{K_{25}}{K_{24}}\Big]$$

$$+ 2za\Big[\tan^{-1}U_{14} + \tan^{-1}U_{24} + \tan^{-1}\Big(\frac{S_4}{z}\Big)$$

$$- \tan^{-1}U_{15} - \tan^{-1}U_{25} - \tan^{-1}\Big(\frac{S_5}{z}\Big)\Big]\Big\}$$

$$
\begin{aligned}
&- \frac{v_x j}{2}\Bigg\{x \ln \frac{Q_{14}Q_{24}g_5}{Q_{15}Q_{25}g_4} + f_1 \ln \frac{K_{14}}{K_{15}} + f_2 \ln \frac{K_{24}}{K_{25}} \\
&- 2z\Bigg[\tan^{-1} U_{15} - \tan^{-1} U_{14} + \tan^{-1} U_{25} - \tan^{-1} U_{24} \\
&+ \tan^{-1}\left(\frac{S_5}{z}\right) - \tan^{-1}\left(\frac{S_4}{z}\right)\Bigg]\Bigg\} \\
&- v_y j\Bigg\{Q_{14} + Q_{15} + Q_{24} + Q_{25} - 2Q_{13} - 2Q_{23} \\
&+ x \ln \frac{K_{13}^2 K_{23}^2}{K_{14}K_{24}K_{15}K_{25}} + a \ln \frac{K_{14}K_{24}}{K_{15}K_{25}}\Bigg\}\Bigg\}
\end{aligned}
\tag{3.4}
$$

According to present knowledge, the only permanent electric field existing in the far tail region is the irrotational field directed over the tail from dawn to dusk. This field must be taken into account when the total electric field content of the tail is estimated at the onset of the substorm.

4. *Particle energization*

The kinetic energy of a charged particle changes as it moves through an electromagnetic field. The rate of the energy change can be estimated as

$$dW = \bar{F} \cdot d\bar{s} \tag{4.1}$$

where $\bar{F}$ is the Lorentz force acting on the particle, and $d\bar{s}$ is an infinitesimal distance along the particle trajectory. Only the electric Lorentz force acts on particles because $\bar{v} \times \bar{B} \cdot d\bar{s} = 0$. Hence only an electrostatic field or a rotational electric field due to changes in the magnetic field is able to change the energy of a charged particle.

Our model includes both magnetic and electric fields changing in time. To study particle energization, we must know the movement of a given particle and the temporary electric field components at each point on its trajectory during a given time interval. So in a computer simulation, three main problems must be taken into account: 1) the change of the particle velocity, 2) the change of the electromagnetic fields, and 3) the change of the particle mass (mainly as regards electrons). All these affect the length of the integration step along the trajectory of the particle.

Since guiding-centre approximation does not give the real particle trajectory, and may even be non-valid in some regions of the tail, the only way to treat the movement of the particle is to start from the relativistic equation of motion:

$$\frac{d}{dt}(m\dot{\bar{r}}) = q\bar{E}(\bar{r}, t) + q\dot{\bar{r}} \times \bar{B}(\bar{r}, t) \tag{4.2}$$

This can be written in component form

$$\dot{x} = u, \quad \dot{y} = v, \quad \dot{z} = w$$

$$\frac{d}{dt}(mu) = qE_x + q(vB_z - wB_y)$$

$$\frac{d}{dt}(mv) = qE_y + q(wB_x - uB_z) \tag{4.3}$$

$$\frac{d}{dt}(mw) = qE_z + q(uB_y - vB_x)$$

where $m = \gamma m_0$, $\gamma = \left(1 - \frac{u^2 + v^2 + w^2}{c^2}\right)^{-1/2}$

So *e.g.*

$$\frac{d}{dt}(mu) = \gamma^2 m\left\{\frac{uv\dot{v} + uw\dot{w}}{c^2} + \dot{u}\left(1 - \frac{v^2 + w^2}{c^2}\right)\right\} \tag{4.4}$$

Making the following transformation

$$\frac{u}{c} \to u, \quad \frac{v}{c} \to v, \quad \frac{w}{c} \to w, \quad ct \to t \tag{4.5}$$

we can write equations (4.3) in the forms

$$\dot{x} = u, \quad \dot{y} = v, \quad \dot{z} = w$$

$$\begin{aligned}
0 &= (1 - v^2 - w^2)\,\dot{u} + uv\dot{v} + uw\dot{w} - \alpha\left(\frac{E_x}{c} + vB_z - wB_y\right) \\
0 &= vu\dot{u} + (1 - u^2 - w^2)\,\dot{v} + vw\dot{w} - \alpha\left(\frac{E_y}{c} + wB_x - uB_z\right) \\
0 &= wu\dot{u} + wv\dot{v} + (1 - u^2 - v^2)\,\dot{w} - \alpha\left(\frac{E_z}{c} + uB_y - vB_x\right),
\end{aligned} \tag{4.6}$$

where $\alpha = \frac{q}{m_0 c}(1 - u^2 - v^2 - w^2)^{3/2}$.

$\dot{u}$, $\dot{v}$, and $\dot{w}$ can be solved from the last three equations. As a result we get a set of differential equations

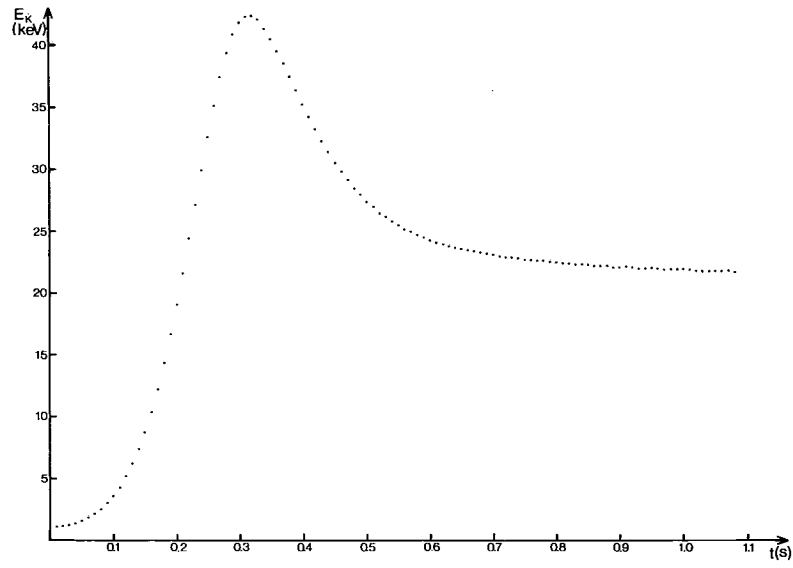

Figure 3. Kinetic energy gained by an electron from the parallel component of the induced electric field in the palsma sheet above and below the neutral sheet. The initial gain in energy is due to the negative meander, and the subsequent loss is due to the positive meander on the dusk side.

$$\begin{aligned} \dot{x} &= u, \quad \dot{y} = v, \quad \dot{z} = w \\ \dot{u} &= \dot{u}(x, y, z, u, v, w) \\ \dot{v} &= \dot{v}(x, y, z, u, v, w) \\ \dot{w} &= \dot{w}(x, y, z, u, v, w), \end{aligned} \tag{4.7}$$

which can be solved numerically by the fourth-order Runge-Kutta method (*e.g.* FRÖBERG [8]). Time dependence can be taken into account by calculating new field values for each point along the particle trajectory at a basic time interval of 10^{-4} seconds; the time interval must be decreased gradually in the relativistic region to keep the numerical method valid.

For practical computations we have to know the initial location (x, y, z), kinetic energy and pitch angle of the particle. If we wish to study its field-aligned acceleration, we can use the total electromagnetic field of our model and trace the motion of the particle according to equations (4.7). Figure 3 shows an example of the longitudinal acceleration of an electron originally with a pitch angle of 90°, launched close to the neutral sheet in a region where the induced

E_x component is large. The electron first reaches nearly 50 keV over the negative meander on the evening side; but if the positive meander is equally strong, the electron encounters some deceleration before it leaves the region of the disturbance toward the earth. Not all of its energy is lost, however, owing to the divergence of the magnetic field lines away from the neutral sheet, and the consequent attenuation of the induced electric field. In this example the electron reaches the plane at the point where $x = -20\,R_E$ with 21 keV.

For betatron acceleration we must use the electric field and B_z in our model. Our main interest is in tracing particles with a pitch angle of 90° in the neutral sheet. For practical reasons (discontinuity in $\bar{B}$ where $z = 0$) we have to make the analysis on some plane close to the neutral sheet, *e.g.* where $z = 0.1$ Re, and drop the B_x and B_y components. Examples of numerical calculations are given in PELLINEN and HEIKKILA [16].

5. *Parameter representation and numerical results*

The disturbed magnetic field (equations 2.7...2.9) and induced electric field (equations 3.3 and 3.4), include six different parameters, whose values have to be obtained by observation. These parameters are the geometrical parameters a and b, current parameters $\partial j/\partial t$ and j, and velocity parameters v_x and v_y.

From numerical computations, we wish to obtain the electric field values in the equation mV/m = 10^{-3} V/m, and the magnetic field values in nT = 10^{-9} Vs/m^2.

Formulas (2.7...2.9) include the coefficient $\mu_0 j/4\pi$, giving the order of magnitude of the magnetic field. By definition:

$$\frac{\mu_0}{4\pi} = 10^{-7}\,\frac{\mathrm{Tm}}{\mathrm{A}}\,.$$

This means that if we insert the current values around $10^{-2}\,\frac{\mathrm{A}}{\mathrm{m}}$, we get magnetic fields of the order of nT. In the computer treatment we use

$$j = \langle j \rangle\, 10\,\frac{\mathrm{mA}}{\mathrm{m}} \tag{5.1}$$

where $\langle j \rangle$ is a dimensionless number defining the value of the current. Since the cross-tail current in the far tail region is typically 10...25 mA/m (depending on the model and nature of the substorm), we can safely say that $\langle j \rangle$ is less than 10, assuming the disturbance current is of the same order of magnitude.

For the geometrical parameters we use one earth radius R_E as the scale, hence

$$a = \langle a \rangle \, R_E$$
$$b = \langle b \rangle \, R_E \tag{5.2}$$

R_E is not usually needed explicitly, except in the $\partial j/\partial t$ terms of the electric field components. For instance, E_y in equation (3.4) must be treated in the following way

$$E_y = \frac{\mu_0}{4\pi a}\left(-\frac{\partial j}{\partial t} + \frac{v_x j}{2a}\right) \quad [\ldots \text{ dimension } R_E^2 \ldots]$$
$$= \frac{\mu_0}{4\pi}\left(-\frac{\partial j}{\partial t}\, a + \frac{v_x j}{2}\right)\frac{1}{a^2} \quad [\text{dimension } R_E^2 \ldots]$$

where $\dfrac{\mu_0}{4\pi}\dfrac{\partial j}{\partial t}\, a = \dfrac{\mu_0}{4\pi}\left\langle\dfrac{\partial j}{\partial t}\right\rangle 10\,\dfrac{\text{mA}}{\text{ms}}\,\langle a \rangle R_E$

$$= \left\langle\frac{\partial j}{\partial t}\right\rangle \langle a \rangle \, 6.37\,\frac{\text{mV}}{\text{m}}$$

where $\left\langle\dfrac{\partial j}{\partial t}\right\rangle$ and $\langle a \rangle$ are dimensionless numbers.

According to the above analysis, the correct magnitude for the electric field will be obtained if we use

$$\frac{\partial j}{\partial t} = \left\langle\frac{\partial j}{\partial t}\right\rangle 6.37 \tag{5.3}$$

in the numerical computations. The magnitude of $\left\langle\dfrac{\partial j}{\partial t}\right\rangle$ can be estimated from magnetic field observations in the velocity independent approximation

$$\bar{B} = \nabla \times \bar{A} \quad \text{and hence} \quad \frac{\partial \bar{B}}{\partial t} = \nabla \times \frac{\partial \bar{A}}{\partial t}$$

$$\frac{\dfrac{\partial \bar{B}}{\partial t}}{\bar{B}} = \frac{\nabla \times \dfrac{\partial \bar{A}}{\partial t}}{\nabla \times \bar{A}} = \frac{\nabla \times \dfrac{\partial j}{\partial t}\dfrac{\partial \bar{A}(\bar{r}, t)}{\partial j}}{\nabla \times j\,\dfrac{\partial \bar{A}(\bar{r}, t)}{\partial j}} = \frac{\dfrac{\partial j}{\partial t}}{j}$$

where

$$\bar{A}(\bar{r}, t) = j(t)\,\bar{A}(\bar{r}) \quad \text{and hence} \quad \bar{A}(\bar{r}) = \frac{\partial \bar{A}(\bar{r}, t)}{\partial j}$$

In the model calculations we can start from the assumption that the cross-tail current in a local region of the tail drops to zero in time Δt. In our earlier paper (PELLINEN [15]) we assumed that the current density (J = 26 mA/m when

$x = -30\,R_E$) decreased to zero in 20 seconds. Hence $\partial j/\partial t = 0.13$ x 10 mA/ms. This corresponds to $\partial B/\partial t = 6$ nT/min in the neutral sheet (where B is typically around 2 nT), which is in fair agreement with observations.

The plasma flow velocity terms of $\vec{E}$ have coefficients $(\mu_0/4\pi)\, vj$. If we choose the formula

$$v = \langle v \rangle\, 10^6\, \frac{\mathrm{m}}{\mathrm{s}}, \tag{5.4}$$

we get

$$\frac{\mu_0}{4\pi}\, vj = \langle j \rangle\, 10^{-9}\, \frac{\mathrm{Vs}}{\mathrm{m}^2}\, \langle v \rangle\, 10^6\, \frac{\mathrm{m}}{\mathrm{s}}$$

$$= \langle j \rangle \langle v \rangle \frac{\mathrm{mV}}{\mathrm{m}}$$

Since the observed flow velocities in the magnetotail vary from 0 to 1500 km/s, $\langle v \rangle$ will obtain values between 0 and 1.5.

In energization problems the unit of length is R_E and speed is given in velocity of light. Hence we use the following unit of time:

$$\tau = ct = 3 \text{ x } 10^8\, \frac{\mathrm{m}}{\mathrm{s}} \text{ x s} = 47.0883\ R_E$$

$$\tau = \langle \tau \rangle \text{ x } 47.0883\ R_E \tag{5.5}$$

$\langle \tau \rangle$ is a dimensionless number expressing the number of seconds counted during the acceleration.

In our previous papers (PELLINEN and HEIKKILA [16], and PELLINEN [15]) we gave numerical results on magnetic and electric field values. We also described the temporal development of neutral line regions and the growth of particle energy in certain simulations. Here we return to this topic and give further details on the electromagnetic field structure, mainly around the neutral line in the equatorial plane (actually on the planes $Z = 1\ R_E$ and $Z = 0.1\ R_E$ owing to the difficulties due to discontinuity discussed earlier in this paper).

Figure 4 gives the isocontours of the disturbance field B_z on the plane where $Z = 1\ R_E$, 15 seconds after the onset of the substorm. The current disturbance is shown by the rectangular dotted line. The current density j_x is 6.5 mA/m and in the middle of the disturbance and 32.5 mA/m on the outer borders. A typical feature of the magnetic flux produced by the loop-type currents can be seen in figure 4: the flux is very dense inside the loop; outside the loop the density is one order of magnitude lower.

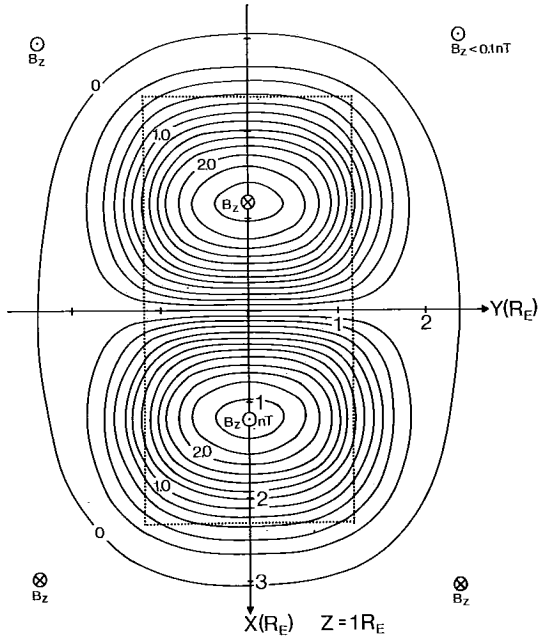

Figure 4. Isocontours of B_z at $Z = 1\ R_E$. The current disturbance is indicated by the rectangular dotted line.

Figure 5a shows values of the electric field E_y in the same situation as above, where $\frac{\partial j}{\partial t}$ is $1.3\ \frac{\text{mA}}{\text{ms}}$. In the middle, the direction of E_y is dawn-to-dusk, and its value is $3.0\ \frac{\text{mV}}{\text{m}}$. At both ends of the area of the disturbance, E_y is reversed and its values are $1.2\ \frac{\text{mV}}{\text{m}}$. These values can be compared with typical cross-tail electric field values in the literature (*e.g.* AKASOFU [1]). These are less than 1 mV/m, usually between 0.2 and 0.5 mV/m. The induction mechanism gives values of several mV/m over a large area in the plasma sheet, which means that the static cross-tail electric field is negligible compared to the induction field at the onset of the substorm.

Figure 5b gives the corresponding values of E_x. These electric-field values can be projected along magnetic field lines. This means that in regions where $E_\parallel$ points earthwards, it accelerates protons in that direction, and in regions where $E_\parallel$ points tailwards, it accelerates electrons towards the earth (Figure 6). The field maxima are displaced outside the dubble region owing to the expansion of the disturbance towards the dawn and dusk side. (Tailward and earthward in Figure 5a).

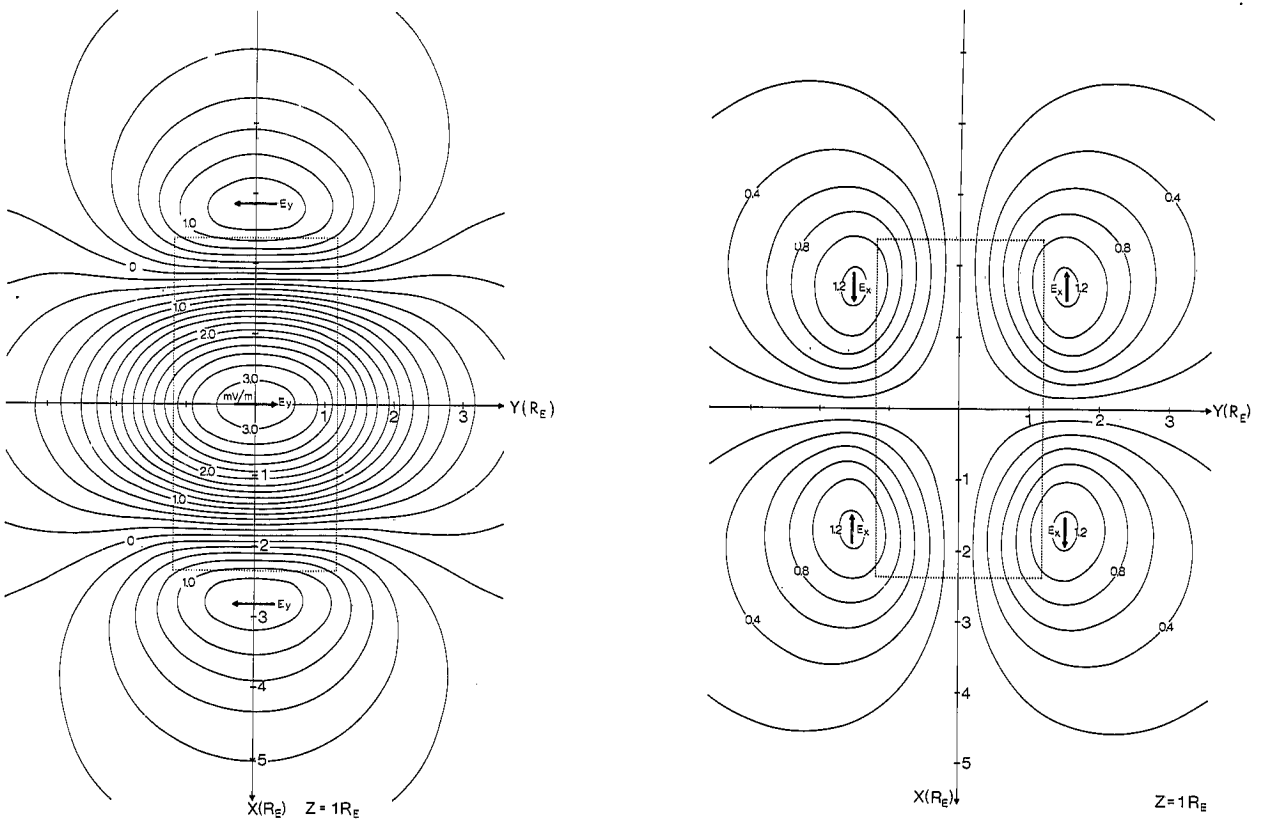

Figures 5a and b. E_y and E_x depicted when $Z = 1\ R_E$. The outward shifts of the field maxima are due to the expansion of the disturbance.

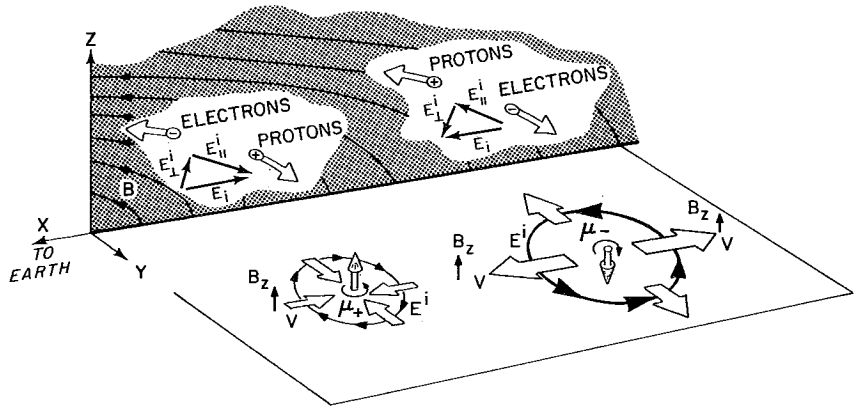

Figure 6. The parallel component of induced electric field $E_\parallel$ in tail lobes accelerates protons and electrons on the dawnside and duskside of the perturbation; only the dawnside is shown, the directions are reversed on the duskside. The magnetic moments of positive and negative meanders are as shown.

By inserting the disturbance in the tail model given in equations (2.10)...(2.12) we obtain the structure of the neutral line on the equatorial plane. Figure 7a shows the magnetic and electric field strengths in the region of the negative current meander when $Z = 0.1\,R_E$, $t = 15$ seconds and $\partial B/\partial t = 0.17$ nT/s. The region with negative B_z is surrounded by a neutral line, with X-type geometry near where $x = -30\,R_E$ and the current strength is decreasing, and 0-type geometry on the other three sides where the current is increasing.

Figure 7b shows the components of the induced electric field on the plane of the neutral sheet ($Z = 0.1\,R_E$), relative to the neutral line in the negative meander. It is interesting to note that, in some regions inside the neutral line, we can draw circles along which the electric field components are always directed in the same tangential direction. This supports our idea that betatron acceleration occurs close to the neutral-line region. Regions causing linear acceleration can also be found. Examples of particle patterns and acceleration magnitudes are given in PELLINEN and HEIKKILA [16].

6. *Discussion*

In this paper we have mainly considered a mathematical model valid during the first few seconds at the onset of a magnetospheric substorm. We have not dealt with the process that triggers this type of disturbance: the basic physics of the plasma processes causing the disturbance remain a problem to be tackled in

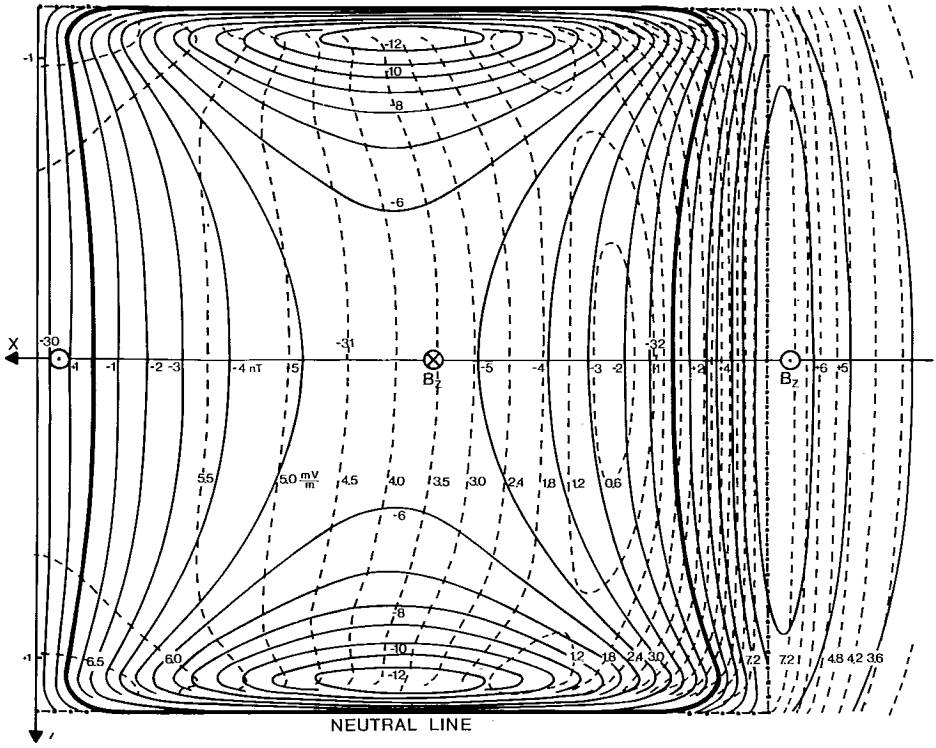

Figure 7a. Magnetic and electric field strengths of the perturbation around the negative current meander, when t = 15 seconds and $\partial B/\partial t$ = 0.17 nT/s. The region with negative B_z is surrounded by a neutral line, with X-type geometry near the point where $X = -30$ R_E and the current strength is decreasing, and O-type geometry on the other three sides where the current is increasing.

the future. Instead, we have jumped right into the middle of the problem. Even so, this ad-hoc model reveals significant features, such as topological features in three dimensions and an explicit time dependence that must be taken into account in the development of physically more realistic models.

As stated in the Introduction, we believe, we have used all essential observations as the starting point for deriving our model. We have taken good care to see that the model does not disagree with present observations of phenomena connected with the onset of substorms.

The model is three-dimensional and time-dependent. Most earlier models on substorms have been two-dimensional (see *e.g.* AKASOFU [1] for a review), so they have not been able to explain the formation of Birkeland currents. The lack of time dependence in earlier models has been an even greater problem than their

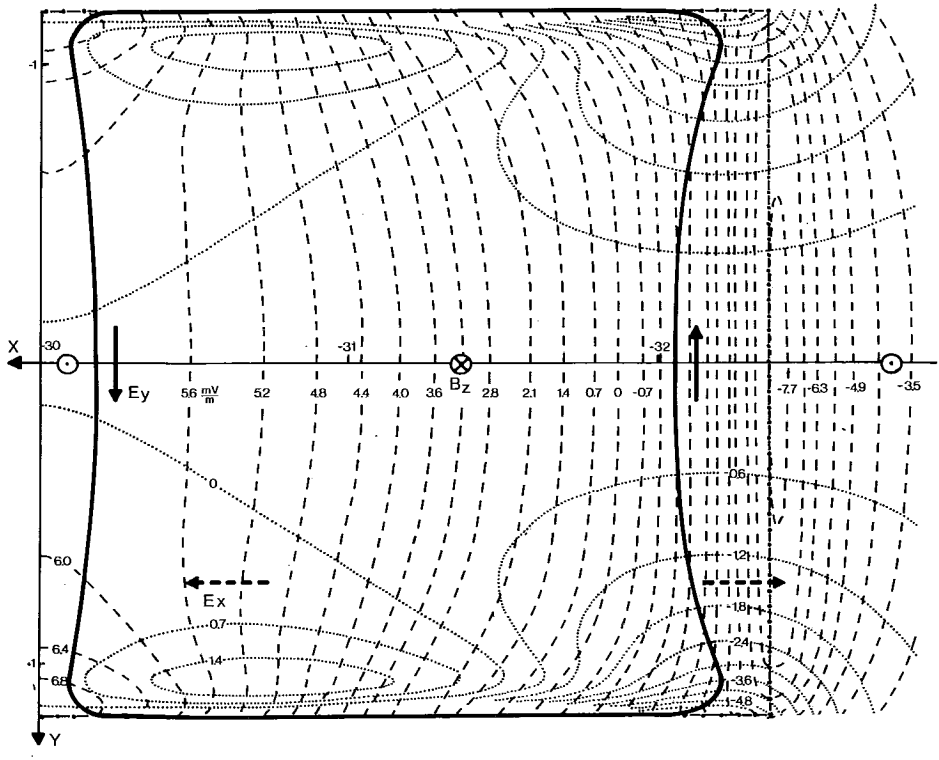

Figure 7b. Components of the induced electric field on the plane of the neutral sheet, relative to the neutral line in the negative meander.

two-dimensionality, because that is obviously disagrees with observations. In any plausible substorm model, account must be taken of $\partial \bar{B}/\partial t$, and thus of the induced electric field, which differs significantly from static fields. At the moment of onset it is obvious that $\bar{E}^i$ is the most important, so all other electric fields can be disregarded.

The model is analytical, which means that numerical calculations can be done quickly and easily on a computer. At this stage, it is not sensible to introduce more complex current patterns, because the lack of a suitable model for the tail at the moment of onset makes it premature to consider physically realistic situations. Largely for this reason the model is not self-consistent. In other words the mechanism that sustains the disturbance is not explained, and the plasma flow parameters are not matched with the electromagnetic field values.

From the above it is obvious that a physically more realistic model must be found, either by means of a satisfactory theory, or empirically, basing on more

detailed observations. Nevertheless, we believe that our model does include the essential features. At this stage, owing to the wide variability of the actual events being studied, the quantitative aspect is not as important as the qualitative.

Acknowledgement: I am grateful to the University of Texas at Dallas and to Sohlberg Committee of the Finnish Scientific Society for supporting this work financially. I also wish to express my gratitude to W. Heikkila for suggesting this problem and for fruitful discussions, and to P. Welling for preparing the computer programs and plots for this work.

REFERENCES

1. AKASOFU, S.-I., 1971: *Physics of Magnetospheric Substorms. 47.* Dordrecht-Holland/ Boston-U.S.A., D. Reidel Publishing Company, 599 p.
2. ARNOLDY, R.L., 1974: Auroral particle precipitation and Birkeland currents. *Rev. Geophys. Space Phys.* **12**, 217.
3. BAKER, D.N. and E.C. STONE, 1976: Energetic Electron Anisotropies in the Magnetotail: Identification of Open and Closed Field Lines. *Geophys. Res. Letters* 3, 557.
4. BEARD, D.B., BIRD, M. and Y.H. HUANG, 1970: Self-consistent theory of the magnetotail. *Planet. Space Sci.* **18**, 1349–1355.
5. BIRD, M.K. and D.B. BEARD, 1972: The self-consistent geomagnetic tail under static conditions. *Ibid.*, **20**, 2057–2072.
6. BOSTRÖM, R., 1964: A model of the auroral electrojets. *J. Geophys. Res.* **69**, 4983.
7. FRANK, L.A., ACKERSON, K.L. and R.P. LEPPING, 1976: On Hot Tenuous Plasmas, Fireballs, and Boundary Layers in the Earth's Magnetotail. *Ibid.* **81**, 5859.
8. FRÖBERG, C.-E., 1969: *Introduction to numerical analysis.* 2nd ed. Reading Mass., 433.
9. FUKUNISHI, H., 1975: Dynamic relationship between proton and electron auroral substorms. *J. Geophys. Res.* **80**, 553.
10. HEIKKILA, W.J. and R.J. PELLINEN, 1977: Localized inductive electric field within the magnetotail. *Ibid.*, **82**, 1610–1613.
11. HONES, E.W., PALMER, I.D. and P.R. HIGBIE, 1976: Energetic Protons of Magnetospheric Origin in the Plasma Sheet Associated With Substorms. *Ibid.* **81**, 3866.
12. HONES, E.W., BAME, S.J. and J.R. ASBRIDGE, 1976: Proton Flow Measurements in the Magnetotail Plasma Sheet Made With Imp 6. *Ibid.* **81**, 227.
13. KIRSCH, E., KRIMIGIS, S.M., SARRIS, E.T., LEPPING, R.P. and T.P. ARMSTRONG, 1977: Possible Evidence For Large, Transient Electric Fields in the Magnetotail from Oppositely Directed Anisotropies of Energetic Protons and Electrons. *Geophys. Res. Lett.* **4**, 137–140.
14. MURPHY, C.H., WANG, C.S. and J.S. KIM, 1975: Inductive Electric Field of a Time-Dependent Magnetotail Current. *Ibid.* **2**, 165.
15. PELLINEN, R.J., 1978: Model for the onset of a magnetospheric substorm. Accepted for publication in *Planet. Space Sci.*
16. PELLINEN, R.J. and W.J. HEIKKILA, 1977: Energization of charged particles to high energies by an induced substorm electric field within the magnetotail. *J. Geophys. Res.* **83**, 1544–1550.

17. ROSTOKER, G. and F.P. CAMIDGE, 1971: Localized character of magnetotail magnetic fluctuations during polar magnetic substorms. *Ibid.* **76**, 6944.

18. SARRIS, E.T., KRIMIGIS, S.M. and T.P. ARMSTRONG, 1976: Observations of Magnetospheric Bursts of High-Energy Protons and Electrons at 35 R_E With Imp 7. *Ibid.* **81**, 2341.

19. SARRIS, E.T., KRIMIGIS, S.M., IIJIMA, T., BOSTROM, C.O. and T.P. ARMSTRONG, 1976: Location of the Source of Magnetospheric Energetic Particle Bursts by Multi-spacecraft Observations. *Geophys. Res. Lett.* **3**, 437.

20. TERASAWA, T. and A. NISHIDA, 1976: Simultaneous Observations of Relativistic Electron Bursts and Neutral-Line Signatures in the Magnetotail. *Plan. Space Sci.* **24**, 855.